

# Evidence for nuclear gluon shadowing from the ALICE measurements of PbPb ultraperipheral exclusive $J/\psi$ production

V. Guzey<sup>a</sup>, E. Kryshen<sup>a</sup>, M. Strikman<sup>b</sup>, M. Zhalov<sup>a</sup>

<sup>a</sup>*National Research Center “Kurchatov Institute”, Petersburg Nuclear Physics Institute (PNPI), Gatchina, 188300, Russia*

<sup>b</sup>*The Pennsylvania State University, University Park, PA 16802, USA*

---

## Abstract

We show that the recent ALICE measurements of exclusive  $J/\psi$  production in ultraperipheral PbPb collisions at 2.76 TeV provide the first direct experimental evidence for the strong nuclear gluon shadowing in lead at  $x \sim 10^{-3}$ . The evidence is based on the comparison of the nuclear suppression factor  $S(x \approx 0.001) = 0.61^{+0.05}_{-0.04}$  found in the analysis of the coherent  $J/\psi$  photoproduction cross sections measured by ALICE with the nuclear gluon shadowing predicted by the global fits of nuclear parton distributions and by the leading twist theory of nuclear shadowing.

*Keywords:*

ultraperipheral collisions, nuclear shadowing, parton distributions in nuclei

---

## 1. Introduction

This brief communication aims to extract the nuclear suppression of coherent  $J/\psi$  photoproduction off nuclei from the data obtained by the ALICE collaboration in ultra-peripheral PbPb collisions at  $\sqrt{s_{NN}} = 2.76$  TeV at the LHC.

Nucleus–nucleus collisions are considered as ultraperipheral collisions (UPCs), if the impact parameter  $|\vec{b}|$ —the distance between the centers of the colliding nuclei in the transverse plane of the reaction—is larger than the sum of the nuclear radii, i.e.,  $|\vec{b}| > (2 - 3)R_A$ , where  $R_A$  is the nuclear radius (for a review of the UPC physics see, for example, [1]). Hadron interactions are strongly suppressed in such collisions and, thus, experimentally the UPC events are characterized by minimal multiplicity. This results in a relative enhancement of electromagnetic processes induced by the high flux of photons generated by ultrarelativistic nuclei which scales as  $Z^2$ , where  $Z$  is the charge of the nucleus. The photon virtuality is small and while its transverse momentum is  $\sim 1/R_A$ , its longitudinal momentum is proportional to the large Lorentz factor  $\gamma_L$  of the ion producing the photon flux. Hence, one can apply the method of equivalent photons to express the cross section of  $J/\psi$  production in nucleus–nucleus UPCs as a product of the photon flux emitted by one of the colliding nuclei and the cross section of  $J/\psi$  photoproduction on the other nucleus:

$$\frac{d\sigma_{AA \rightarrow AAJ/\psi}(y)}{dy} = N_{\gamma/A}(y)\sigma_{\gamma A \rightarrow AJ/\psi}(y) + N_{\gamma/A}(-y)\sigma_{\gamma A \rightarrow AJ/\psi}(-y). \quad (1)$$

In Eq. (1),  $N_{\gamma/A}(y) \equiv \omega dN_{\gamma/A}(\omega)/d\omega$  is the photon flux;  $y = \ln(2\omega/M_{J/\psi}) = \ln(W_{\gamma p}^2/(2\gamma_L m_N M_{J/\psi}))$  is the  $J/\psi$  rapidity, where  $\omega$  is the photon energy (in the laboratory frame),  $W_{\gamma p}$  is  $\gamma p$  center-of-mass energy,  $M_{J/\psi}$  is the mass of  $J/\psi$  and  $m_N$  is the nucleon mass. The presence of two terms in Eq. (1) is due to the symmetry of PbPb collisions: each nucleus can radiate a photon as well as serve as a target. The photon flux  $N_{\gamma/A}$  can be calculated with reasonable accuracy and, therefore, the UPCs can be effectively used to study the energy behavior of the vector meson photoproduction cross section at high energies.

High energy coherent  $J/\psi$  photoproduction on nuclei is of a particular interest since the large  $c$ -quark mass,  $m_c$ , provides a hard scale  $\mu \geq m_c$  justifying the use of the factorization theorem of perturbative QCD (pQCD). This allowed one to develop several models predicting the cross section of  $J/\psi$  photoproduction on nuclear targets at high energies. Unfortunately, until recently, the progress in experimental studies of this process was more than modest: about two dozens events have been accumulated in recent measurements of  $J/\psi$  photoproduction in AuAu UPCs at RHIC at  $\sqrt{s_{NN}} = 200$  GeV [2].

In 2011, the ALICE collaboration measured the yield of coherent  $J/\psi$  photoproduction in PbPb UPCs in the rapidity range of  $|y| \leq 0.9$  with the central barrel [3] and in the range of  $-3.6 \leq y \leq -2.6$  covered by the muon spectrometer [4]. This allowed one to obtain the cross section  $\sigma_{PbPb \rightarrow PbPb J/\psi}(y)$  at two values of rapidity:

$$\sigma_{PbPb \rightarrow PbPb J/\psi}(y = 0) \approx 2.38_{-0.24}^{+0.34}(\text{stat.} + \text{syst.}) \text{ mb}, \quad (2)$$

$$\sigma_{PbPb \rightarrow PbPb J/\psi}(y = -3.1) \approx 1.00 \pm 0.18(\text{stat.})_{-0.26}^{+0.23}(\text{syst.}) \text{ mb}. \quad (3)$$

These values of  $\sigma_{PbPb \rightarrow PbPb J/\psi}(y)$  were compared [3, 4] to a number of predictions and appeared to be in a better agreement with those which calculated coherent  $J/\psi$  photoproduction on nuclear targets in the leading order (LO) pQCD taking into account the nuclear gluon shadowing [5, 6].

However, it is reasonable to reduce as much as possible the model dependence in the comparisons of the experimental cross sections with different model calculations. We believe that the best strategy to achieve this goal is to analyze the ALICE results in terms of the nuclear suppression factor  $S(W_{\gamma p})$ . We define  $S(W_{\gamma p})$  through the ratio of the experimentally measured coherent photoproduction cross section at a given  $W_{\gamma p}$  to the cross section calculated in the impulse approximation (IA) which neglects all nuclear effects except for coherence:

$$S(W_{\gamma p}) \equiv \left[ \frac{\sigma_{\gamma Pb \rightarrow J/\psi Pb}^{\text{exp}}(W_{\gamma p})}{\sigma_{\gamma Pb \rightarrow J/\psi Pb}^{\text{IA}}(W_{\gamma p})} \right]^{1/2}. \quad (4)$$

Such a definition of  $S(W_{\gamma p})$  for coherent vector meson photoproduction on nuclear targets corresponds to the standard estimate of nuclear suppression in terms of  $A_{\text{eff}}/A$  [7]. Since the nucleus remains intact in the considered process, the transverse momentum distribution of  $J/\psi$  is dictated by the elastic nuclear form factor  $F_A(t)$ . Hence, the cross section in the impulse approximation can be written as:

$$\sigma_{\gamma Pb \rightarrow J/\psi Pb}^{\text{IA}}(W_{\gamma p}) = \frac{d\sigma_{\gamma p \rightarrow J/\psi p}(W_{\gamma p}, t = 0)}{dt} \Phi_A(t_{\min}). \quad (5)$$

In Eq. (5),  $d\sigma_{\gamma p \rightarrow J/\psi p}(W_{\gamma p}, t = 0)/dt$  is the forward differential cross section of  $\gamma + p \rightarrow J/\psi + p$  which can be extracted from the experimental data [8];  $\Phi_A(t_{\min})$  is defined as the integral over the

nuclear form factor  $F_A(t)$  squared:

$$\Phi_A(t_{\min}) = \int_{t_{\min}}^{\infty} dt |F_A(t)|^2, \quad (6)$$

where  $t_{\min} = -p_{z,\min}^2 = -[M_{J/\psi}^2/(4\omega\gamma_L)]^2$  is determined by the minimal longitudinal momentum transfer  $p_{z,\min}$  characterizing the coherence length which becomes important in the low energy domain. In the case of Pb, the nuclear form factor

$$F_A(t) = \int d^2\vec{b} dz e^{i\vec{p}_t \cdot \vec{b}} e^{ip_z z} \rho_A(\vec{b}, z), \quad F_A(0) = A, \quad (7)$$

can be calculated with a small uncertainty since the nuclear density distribution  $\rho_A(\vec{r})$  is well known from the electron–lead and proton–lead elastic scattering experiments [9].

It is important to point out that the suppression factor  $S(W_{\gamma p})$  is practically model independent since the estimate of the cross section in the impulse approximation is based on experimental data.

## 2. Calculation of the suppression factor

### 2.1. Cross section of coherent $J/\psi$ photoproduction in ALICE measurements

In this subsection, we determine the coherent  $J/\psi$  photoproduction cross section  $\sigma_{\gamma Pb \rightarrow J/\psi Pb}(W_{\gamma p})$  from the values of  $\sigma_{Pb Pb \rightarrow Pb Pb J/\psi}(y)$  measured by ALICE. In general, the extraction of  $\sigma_{\gamma Pb \rightarrow J/\psi Pb}(W_{\gamma p})$  is not straightforward due to the presence of two terms in Eq. (1). However, this problem is not present at  $y = 0$  since the energies of the photons emitted by both colliding ions are equal in this case. Thus, we obtain:

$$\sigma_{\gamma Pb \rightarrow J/\psi Pb}(W_{\gamma p} = 92.4 \text{ GeV}) = \frac{\sigma_{Pb Pb \rightarrow Pb Pb J/\psi}(y = 0)}{2N_{\gamma/Pb}(y = 0)}. \quad (8)$$

On the other hand, at forward rapidity  $y = -3.1$ , there are low-energy and high-energy contributions. Calculations predict the strong dominance of the low-energy contribution (more than 95%) in Eq. (1) due to a steep falloff of the photon flux for high photon energies. Therefore, in this case we obtain:

$$\sigma_{\gamma Pb \rightarrow J/\psi Pb}(W_{\gamma p} = 19.6 \text{ GeV}) = \frac{\sigma_{Pb Pb \rightarrow Pb Pb J/\psi}(y = -3.1)}{N_{\gamma/Pb}(y = -3.1)}, \quad (9)$$

which is valid with a 5% error that is well below the experimental uncertainties.

Next we need to calculate the photon flux  $N_{\gamma/Pb}(y)$  produced by Pb nuclei with the energy of 1.38 ATeV. Experimentally, coherent  $J/\psi$  events are selected by requiring only two daughter leptons and the otherwise empty detector. This means that the strong interactions between colliding nuclei should be suppressed and, hence, the impact parameter is required to be larger than the sum of the nuclear radii:  $b > 2R_A$ . Actually, the sharp cutoff at  $2R_A$  can be improved by using

a more accurate approximation in the calculation of the strong interaction suppression. Indeed, using the profile factor

$$\Gamma_{AA}(\vec{b}) = \exp\left(-\sigma_{NN} \int_{-\infty}^{\infty} dz \int d^2\vec{b}_1 \rho_A(z, \vec{b}_1) \rho_A(z, \vec{b} - \vec{b}_1)\right), \quad (10)$$

where  $\sigma_{NN} = 80$  mb is the total nucleon–nucleon ( $NN$ ) cross section at  $\sqrt{s} = 2.76$  TeV [10], the photon flux can be calculated as the following convolution:

$$N_{\gamma/A}(\omega) = \int_{2R_A}^{\infty} d^2\vec{b} \Gamma_{AA}(\vec{b}) N_{\gamma/A}(\omega, \vec{b}). \quad (11)$$

The photon flux at the transverse distance (impact parameter)  $\vec{b}$  from the center of a fast moving heavy nucleus reads, see, e.g., [11]:

$$N_{\gamma/A}(\omega, \vec{b}) = \frac{Z^2\alpha}{\pi^2} \left| \int_0^{\infty} dk_{\perp} \frac{k_{\perp}^2 F_A(k_{\perp}^2 + \omega^2/\gamma_L^2)}{k_{\perp}^2 + \omega^2/\gamma_L^2} J_1(bk_{\perp}) \right|^2, \quad (12)$$

where  $\alpha$  is the fine-structure constant;  $J_1$  is the Bessel function of the first kind.

Using Eqs. (10)–(12), we obtain the following values of the photon flux:

$$\begin{aligned} N_{\gamma/Pb}(y=0) &= 67.7 \pm 3.4, \\ N_{\gamma/Pb}(y=-3.1) &= 163.9 \pm 8.2. \end{aligned} \quad (13)$$

The quoted uncertainties were estimated by utilizing different nuclear density distributions in the calculation of the nuclear form factor and the profile factor.

Using Eqs. (8) and (9), the values of the cross sections measured by ALICE [Eqs. (2) and (3)] and our estimates of the photon flux [Eq. (13)], we obtain the following values of the  $J/\psi$  photoproduction cross section:

$$\begin{aligned} \sigma_{\gamma Pb \rightarrow J/\psi Pb}(W_{\gamma p} = 92.4 \text{ GeV}) &= 17.6_{-2.0}^{+2.7} \mu\text{b}, \\ \sigma_{\gamma Pb \rightarrow J/\psi Pb}(W_{\gamma p} = 19.6 \text{ GeV}) &= 6.1_{-2.0}^{+1.8} \mu\text{b}, \end{aligned} \quad (14)$$

where the experimental errors and the flux uncertainty were added in quadrature.

## 2.2. $J/\psi$ photoproduction on $Pb$ in the impulse approximation

To determine the nuclear suppression factor  $S(W_{\gamma p})$  from Eq. (4), we need to calculate the coherent  $J/\psi$  photoproduction cross section in the impulse approximation,  $\sigma_{\gamma Pb \rightarrow J/\psi Pb}^{\text{IA}}(W_{\gamma p})$ , which is given by Eq. (5).

The forward differential  $\gamma + p \rightarrow J/\psi + p$  cross section at  $W_{\gamma p} = 19.6$  GeV and  $W_{\gamma p} = 92.4$  GeV can be extracted from HERA, FNAL and CERN measurements [8]<sup>1</sup>. A compilation

---

<sup>1</sup> Exclusive  $J/\psi$  production has been measured at  $y = 0$  in ultraperipheral  $p\bar{p}$  collisions by the CDF collaboration at Tevatron [12]. The  $\gamma p \rightarrow J/\psi p$  cross section obtained from their value of  $\sigma_{p\bar{p} \rightarrow p\bar{p} J/\psi}(y = 0)$  is in reasonable agreement with the HERA measurements. Recently, the LHCb collaboration measured the yield of  $J/\psi$  at the forward rapidities of  $2 < y < 4.5$  in proton–proton UPCs at 7 TeV [13]. This data allowed one to extract the  $\gamma p \rightarrow J/\psi p$  cross section at the  $\gamma p$  center-of-mass energies of  $0.6 \text{ TeV} < W_{\gamma p} < 1 \text{ TeV}$ .

of the experimental results is shown in Fig. 1. The  $10 \text{ GeV} < W_{\gamma p} < 25 \text{ GeV}$  range of energies corresponding to the ALICE muon spectrometer acceptance in the measurement of  $J/\psi$  production in PbPb UPCs at 2.76 TeV was studied in the old proton-target experiments at FNAL and CERN. Statistics in those experiments was very low resulting in large experimental errors. The forward  $J/\psi$  photoproduction cross section at higher energies was measured by the H1 and ZEUS collaborations at HERA. As can be seen in Fig. 1, the cross sections measured by these two experiments do not agree well, with the most recent H1 measurement being systematically higher over the entire energy range.

The data in Fig. 1 was fitted using the following pQCD motivated expression [14]:

$$\frac{d\sigma_{\gamma p \rightarrow J/\psi p}(W_{\gamma p}, t=0)}{dt} = C_0 \left[ 1 - \frac{(M_{J/\psi} + m_N)^2}{W_{\gamma p}^2} \right]^{1.5} \left[ \frac{W_{\gamma p}^2}{100^2 \text{ GeV}^2} \right]^\delta, \quad (15)$$

The values of the free parameters  $C_0$  and  $\delta$  were determined from the fit, resulting in  $C_0 = 342 \pm 8 \text{ nb/GeV}^2$  and  $\delta = 0.40 \pm 0.01$ . Then, the corresponding values of the forward cross section are:

$$\begin{aligned} \frac{d\sigma_{\gamma p \rightarrow J/\psi p}(19.6 \text{ GeV}, t=0)}{dt} &= 86.9 \pm 1.8 \text{ nb/GeV}^2, \\ \frac{d\sigma_{\gamma p \rightarrow J/\psi p}(92.4 \text{ GeV}, t=0)}{dt} &= 319.8 \pm 7.1 \text{ nb/GeV}^2. \end{aligned} \quad (16)$$

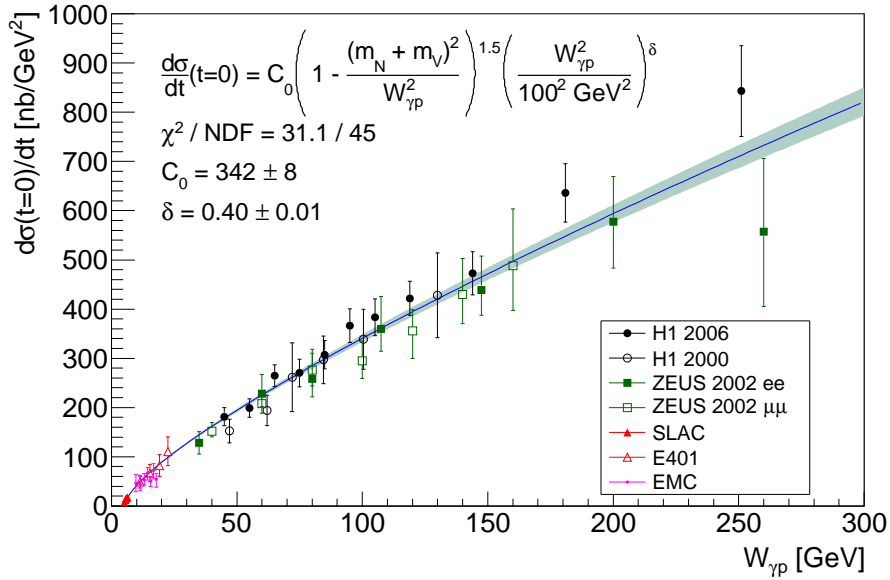


Figure 1: The fit to the forward  $J/\psi$  photoproduction cross section data [8].

To calculate  $\Phi_A(t_{\min})$  and to estimate its uncertainty, we evaluate  $\Phi_A(t_{\min})$  using three different nuclear form factors. In particular, we used the analytic parametrization of  $F_{\text{Pb}}(t)$  from StarLight [15], which is widely used in analyses of experimental data as a UPC generator. We

also calculated the nuclear form factor using the Hartree–Fock–Skyrme nuclear density distribution  $\rho_{\text{Pb}}(\vec{r})$  and the Woods–Saxon density distribution with the parameters  $R_{\text{Pb}} = 6.62 \pm 0.06$  fm and  $a = 0.546 \pm 0.01$  fm [16]. These distributions provide the good description of the elastic electron–lead and proton–lead scattering data. The three estimates agree within 5% error for both considered energies. In the following calculations, we use the  $\Phi_A(t_{\min})$  values corresponding to the Woods–Saxon density and assign a  $\pm 5\%$  uncertainty:

$$\begin{aligned}\Phi_A(t_{\min}(W_{\gamma p} = 19.6 \text{ GeV})) &= 127.2 \pm 6.4 \text{ GeV}^2, \\ \Phi_A(t_{\min}(W_{\gamma p} = 92.4 \text{ GeV})) &= 149.2 \pm 7.5 \text{ GeV}^2.\end{aligned}\tag{17}$$

Combining Eqs. (5), (16) and (17), we obtain the following values of the  $J/\psi$  photoproduction cross sections in the impulse approximation:

$$\begin{aligned}\sigma_{\gamma \text{Pb} \rightarrow J/\psi \text{Pb}}^{\text{IA}}(W_{\gamma p} = 19.6 \text{ GeV}) &= 11.1 \pm 0.6 \text{ } \mu\text{b}, \\ \sigma_{\gamma \text{Pb} \rightarrow J/\psi \text{Pb}}^{\text{IA}}(W_{\gamma p} = 92.4 \text{ GeV}) &= 47.7 \pm 2.6 \text{ } \mu\text{b},\end{aligned}\tag{18}$$

where the uncertainty of the fit to the forward  $J/\psi$  cross section and the  $\Phi_A(t_{\min})$  uncertainty were added in quadrature.

### 2.3. Estimation of the suppression factor $S(W_{\gamma p})$

Combining Eqs. (4), (14) and (18), we estimate the values of the nuclear suppression factor  $S(W_{\gamma p})$  at the  $W_{\gamma p}$  values corresponding to the ALICE measurements [3, 4]:

$$S(W_{\gamma p} = 19.6 \text{ GeV}) = 0.74_{-0.12}^{+0.11},\tag{19}$$

$$S(W_{\gamma p} = 92.4 \text{ GeV}) = 0.61_{-0.04}^{+0.05}.\tag{20}$$

The dominant part of uncertainties in our estimates comes from the large experimental errors in the measured cross section of  $J/\psi$  production in PbPb UPCs.

## 3. Comparison of the suppression factor with theoretical predictions

The suppression factor  $S(W_{\gamma p})$  that we extracted from the ALICE data can be compared to theoretical predictions for  $S(W_{\gamma p})$  made in different models and approaches.

The earliest approach to the calculation of the cross section of vector meson photoproduction on nuclei is based on the vector meson dominance (VMD) model, see the review in [17]. In this approach, a high energy photon converts into a vector meson at a long distance (time) before the target. Then, the vector meson interacts coherently with the nucleus by means of multiple interactions with the target nucleons. This process of hadron-nucleus interaction is usually described by the Glauber theory. In assumption that the multiple interactions don't distort the shape of the transverse momentum distribution of the vector meson but result only in the absorption effects the suppression factor for coherent vector meson production on the nucleus can be estimated as

$$S_A(W_{\gamma p}) = \frac{\sigma_{VA}(W_{\gamma p})}{A\sigma_{VN}(W_{\gamma p})},\tag{21}$$

$\sigma_{VN}$  is the total vector meson–nucleon cross section. The total vector meson–nucleus cross section  $\sigma_{VA}$  can be calculated in the optical limit of the Glauber theory:

$$\sigma_{VA}(W_{\gamma p}) = 2 \int d^2\vec{b} \left[ 1 - \exp \left\{ -\frac{\sigma_{VN}(W_{\gamma p})}{2} T_A(\vec{b}) \right\} \right], \quad (22)$$

where  $T_A(\vec{b}) = \int_{-\infty}^{\infty} \rho_A(\vec{b}, z) dz$ .

In the case of  $J/\psi$  photoproduction, the application of the VMD approach is problematic because the standard VMD model does not take into account that the space–time picture of production of heavy onium states involves three stages: the production of “frozen” small-size  $q\bar{q}$  configurations, their interaction with the target, and the conversion of  $q\bar{q}$  into the final-state onium. This space–time picture can be modeled using the color dipole framework to calculate the cross section of the interaction of the  $c\bar{c}$  configuration with the nucleon and the Glauber theory (eikonal model) to describe the propagation of the dipoles of the fixed transverse size through the nuclear medium. We estimated the nuclear suppression factor using the phenomenological Golec-Biernat–Wusthoff dipole cross section [18]:

$$\sigma_{VN}(W_{\gamma p}) = \sigma_{c\bar{c}N}(W_{\gamma p}) = \sigma_0 \left[ 1 - \exp \left( -0.25 \langle d \rangle^2 \left( \frac{x_0}{x} \right)^{2\lambda} \right) \right], \quad (23)$$

where  $\langle d \rangle \approx 0.25$  fm is the average size of the  $c\bar{c}$  configuration in  $J/\psi$ ;  $\sigma_0 = 29.12$  mb,  $\lambda = 0.277$  and  $x_0 = 0.000041$  were obtained in [18] from the fit to the nucleon DIS data at small  $Q^2$  and  $x$ . One can see from Eq. (23) that this model assumes a gradual increase of the cross section with a decrease of  $x$  and, hence, an eventual onset of the saturation regime at very small  $x$ .

Figure 2 presents the nuclear suppression factor for lead,  $S_{Pb}(W_{\gamma p})$ , as a function of  $W_{\gamma p}$ . The result of the calculation using Eqs. (21)–(23) is shown by the blue solid line. One can see from the figure that the predicted nuclear suppression is too small compared to the ALICE results, which are shown as two points with the corresponding error bars.

It is worth noting here that for the discussed kinematics, the results for the dipole–nucleon cross section obtained in different dipole models are rather close since they are constrained well by the DIS data for these energies. Note also that in the discussed model, the nuclear shadowing effect is driven by the  $\sigma_{c\bar{c}N}$  dipole cross section and, hence, shadowing is suppressed (a higher twist effect) for the dipoles of such a small size.

One can also estimate the nuclear suppression in the approach used in StarLight generator of ultraperipheral collisions [15]. In StarLight, the total cross section  $\sigma_{J/\psi A}(W_{\gamma p})$  is calculated using the classical probabilistic formula<sup>2</sup>:

$$\sigma_{VA}(W_{\gamma p}) = \int d^2\vec{b} \left[ 1 - \exp \left\{ -\sigma_{VN}(W_{\gamma p}) T_A(\vec{b}) \right\} \right], \quad (24)$$

while the values of  $\sigma_{J/\psi N}(W_{\gamma p})$  are found from the HERA experimental data on  $\gamma p \rightarrow J/\psi p$  cross sections [8] using the VMD model. As a result, the estimated value of  $\sigma_{VN}$  is rather small,

---

<sup>2</sup>Note that the classical probabilistic formula and the Glauber formula give close values of the total  $VA$  cross section only when  $\sigma_{VN} T_A(\vec{b}) \ll 1$ .

which leads to the small nuclear suppression factor  $S_A(W_{\gamma p})$ . Indeed, the prediction for  $S_{\text{Pb}}(W_{\gamma p})$  calculated using Eqs. (21) and (24) with the parameters from StarLight[15], which is shown by the red dashed line in Fig. 2, significantly overestimates the data points that we model-independently extracted from the ALICE data.

It is of particular interest to compare the nuclear suppression found from the analysis of the ALICE data to the corresponding predictions of perturbative QCD. At high energies and small transverse momenta of  $J/\psi$  ( $W_{\gamma p} \gg M_{J/\psi} \gg p_t$ ), in the leading order pQCD, the cross section of coherent  $J/\psi$  photoproduction on the proton is proportional to the proton gluon density  $G_p(x, \mu^2)$  squared [19, 20]:

$$\frac{d\sigma_{\gamma p \rightarrow J/\psi p}(W_{\gamma p}, t=0)}{dt} = C(\mu^2) \left[ x G_p(x, \mu^2) \right]^2, \quad (25)$$

where  $x = M_{J/\psi}^2/W_{\gamma p}^2$  is the fraction of the proton plus-momentum carried by the gluons;  $\mu^2$  is the hard scale. In the approximation that the Fermi motion of the quarks in charmonium is neglected, the prefactor  $C(\mu^2) = M_{J/\psi}^3 \Gamma_{ee} \pi^3 \alpha_s^2(\mu^2)/(48 \alpha_{em} \mu^8)$ , where  $\Gamma_{ee}$  is the width of the  $J/\psi$  electronic decay.

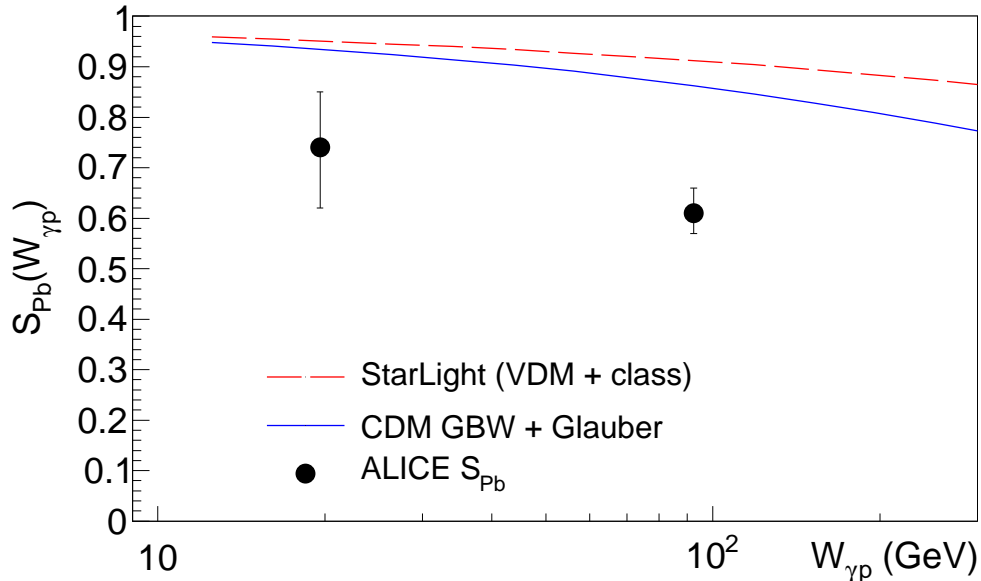


Figure 2: Comparison of the ALICE suppression factors with the estimates in the Glauber model with the color dipole cross section and in the Starlight approach.

It is worth noting that the accuracy of the LO pQCD calculations of the  $J/\psi$  photoproduction cross section is still a subject of discussions, see, e.g., [21, 22, 23]. In particular, the value of the hard scale  $\mu^2$  in the gluon density is not fixed reliably. There are also some uncertainties in estimates of the skewness of the gluon distributions, relativistic effects in the charmonium wave function, and higher order corrections. Some of the corrections increase the cross section, others – suppress it. However, there is a general consent that these effects mainly influence the absolute value of the cross section but not its energy dependence. The total uncertainty of the LO pQCD predictions is estimated in [21, 22] to be about 30% or less, while [23] suggests a larger uncertainty.



Extending Eq. (25) for the description of  $J/\psi$  production on nuclei and accounting for the transverse momentum distribution dictated by the nuclear form factor, one can easily find

$$\sigma_{\gamma A \rightarrow J/\psi A}^{\text{pQCD}}(W_{\gamma p}) = \frac{d\sigma_{\gamma p \rightarrow J/\psi p}(W_{\gamma p}, t=0)}{dt} \left[ \frac{G_A(x, \mu^2)}{AG_N(x, \mu^2)} \right]^2 \Phi_A(t_{\min}). \quad (26)$$

In the impulse approximation,  $G_A(x, \mu^2) = AG_N(x, \mu^2)$  and, hence, the nuclear suppression factor for coherent  $J/\psi$  photoproduction on nuclei is

$$S_A(W_{\gamma p}) = \frac{G_A(x, \mu^2)}{AG_N(x, \mu^2)} \equiv R(x, \mu^2). \quad (27)$$

Hence, in the leading order pQCD, the suppression of coherent  $J/\psi$  photoproduction on nucleus as compared to the impulse approximation results from the coherent nature of the small  $x$  screening of the gluon field of the nucleus which is generally accepted to be characterized by the  $R(x, \mu^2)$  factor<sup>3</sup>.

In the top panel of Fig. 3, we compare the values of  $S(W_{\gamma p})$  obtained in our analysis of the ALICE data (two black solid circles) at  $x = 0.022$  and  $x = 0.001$  corresponding to the energies of  $W_{\gamma p} = 19.6$  GeV and  $W_{\gamma p} = 92.4$  GeV to the  $x$  dependence of the parametrization of the nuclear gluon shadowing factors  $R(x)$  used in HIJING 2.0 generator [24, 25]. In this approach, the nuclear gluon shadowing is characterized by the parameter  $s_g$  and, contrary to pQCD, it does not depend on the scale. In the older version of HIJING [24], the values of  $s_g$  were chosen to be in the range of  $0.24 - 0.28$ . The nuclear gluon shadowing in this case—which is shown by the red dashed curve—is too strong compared to the ALICE suppression factor at  $x \approx 0.001$ . More recent versions of HIJING include the impact parameter dependence of the nuclear gluon shadowing [25] and use the values of  $s_g = 0.17 - 0.22$  determined from fits to the RHIC hadron production data within a two-component mini-jet model. The parametrization with  $s_g \approx 0.18$  describes the ALICE values very well, see the blue solid curve in the top panel of Fig. 3.

In the middle panel of Fig. 3, we compare the nuclear suppression factor found from the analysis of the ALICE data to the  $x$  dependence of the nuclear gluon shadowing factors obtained using several nuclear parton distribution functions (PDFs). These nuclear PDFs are the results of the global QCD fits based on the data on deep inelastic and Drell–Yan processes on nuclei. In particular, we consider HKN07LO [26], nDSLO [27], EPS08LO and EPS09LO [28]. In accordance with [19], we take  $\mu^2 = M_{J/\psi}^2/4$ , which is close to the  $c$ -quark mass squared. Note that a somewhat larger value of  $\mu^2$  is preferred by the analysis of [23].

From the comparison shown in the middle panel of Fig. 3, we see that the HKN07LO, nDSLO and EPS08LO predictions for  $R(x, \mu^2 = 2.4 \text{ GeV}^2)$  are disfavored by the strong contradiction with the nuclear suppression found by ALICE at  $x \approx 0.001$ : while HKN07LO and nDSLO predict too weak shadowing, the EPS08 shadowing is too strong. A good agreement is observed for the central set of the EPS09LO nuclear gluon shadowing factor (blue solid line). However, one has to admit that the uncertainties of EPS09LO (turquoise shaded area) are very large.

---

<sup>3</sup>Note that a consistent treatment within the LO pQCD requires the use of the same proton gluon density  $G_p(x, \mu^2)$  in the calculation of the forward  $\gamma p \rightarrow J/\psi p$  cross section and in the definition of  $R(x, \mu^2)$ .

It is worth noting here that the main problem in the determination of the nuclear gluon shadowing at  $x \sim 10^{-3}$  in the global QCD fit analyses is the lack of high quality data sensitive to the nuclear gluon PDFs not only at these values of  $x$ , but also at larger  $x \approx 0.01$ . As a result, in these fits, almost any values of  $R_A(x \sim 10^{-3}, Q_0^2)$  between 0 and 1 are allowed leading to strong differences between different analyses. Moreover, results of the fits strongly depend on the data selected for a given analysis. In particular, in addition to the DIS and DY data, the EPS08 analysis included in their fit the BRAHMS data [29] on forward high  $p_t$  pion production in dA collisions at RHIC assuming that the nuclear modification of the pion yield in this kinematics is due to the gluon shadowing. This resulted in a very strong effect of nuclear gluon shadowing. However, already in the EPS09 analysis, this data was excluded from the fit since it was difficult to separate the gluon shadowing from other pQCD mechanisms also leading to the suppression of the yield of forward high  $p_t$  pions. Instead, the data on inclusive neutral pion production in dA collisions from PHENIX [30] was added to the DIS and DY data sets in the EPS09 analysis leading to the nuclear shadowing effect which is weaker than that in EPS08, but still stronger than in HKN07 and nDS.

One can also compare the nuclear suppression factor found from the analysis of the ALICE data to the nuclear gluon shadowing factors calculated in the leading twist theory of nuclear shadowing [31]. The latter is a dynamical approach based on the QCD factorization theorems, Gribov's theory [32] of inelastic shadowing corrections in multiple scattering, and the HERA diffractive PDFs [33]. The comparison is presented in the bottom panel of Fig. 3. We show three sets of predictions corresponding to three different sets of the gluon PDF in the free proton. The blue band shows  $R(x, \mu^2 = 2.4 \text{ GeV}^2)$  calculated with the MNRT07LO nucleon gluon density obtained by the Durham-PNPI group [34] from the fit to the HERA data on the coherent photo- and electroproduction of  $J/\psi$  mesons on the proton. The uncertainty of the predicted values of  $R(x, \mu^2 = 2.4 \text{ GeV}^2)$  (the width of the band) reflects the theoretical uncertainty of the leading twist theory associated with the need to model the interactions with  $N \geq 3$  nucleons of the nuclear target.

The red band shows  $R(x, \mu^2 = 2.4 \text{ GeV}^2)$  calculated using the MSTW08LO nucleon gluon density [35]. The resulting value of  $R(x, \mu^2 = 2.4 \text{ GeV}^2)$  is close to the value of nuclear suppression found in the current analysis of the ALICE data at  $x \approx 0.01$ , especially if one takes into account large experimental errors of  $S_{Pb}(x)$ , and agrees well with the ALICE data point at  $x \approx 0.001$ .

Weaker nuclear gluon shadowing (green band) is predicted when one uses the CTEQ6L nucleon gluon distribution.

A word of caution is in order here. In the present comparison with the leading twist approximation (LTA) predictions, we used a particular plausible value of the hard scale  $\mu^2$ ,  $\mu^2 = M_{J/\psi}^2/4 = 2.4 \text{ GeV}^2$ . An increase of  $\mu^2$  (within the allowed limits) will result in weakening of the nuclear gluon shadowing. However, one has to keep in mind that a strong increase of  $\mu^2$  (small gluon shadowing) is disfavored by the comparison with the ALICE suppression factors.

In summary, our analysis shows that the bulk of the nuclear suppression found in the ALICE measurements of  $J/\psi$  photoproduction in UPCs of heavy ions at the LHC energies is due to the nuclear gluon shadowing. Moreover, it seems that a reasonable agreement between the measured nuclear suppression factor with the predictions of nuclear gluon shadowing in the leading twist approximation can be considered as evidence of the adequate description of this phenomenon in the leading twist framework.

## 4. Conclusions

The analysis of the ALICE measurements of exclusive  $J/\psi$  production in ultraperipheral PbPb collisions at 2.76 TeV demonstrates that this data provides the experimental evidence for a comparatively large nuclear suppression in Pb at small  $x \sim 10^{-3}$ . The found values are in agreement with the nuclear gluon shadowing predicted in the framework of leading twist nuclear shadowing and found in the central EPS09LO set of nuclear PDFs.

The significant source of uncertainties comes from experimental errors in the measured cross sections both in exclusive  $J/\psi$  production in PbPb UPCs and in studies of the  $\gamma p \rightarrow J/\psi p$  elementary process. Obviously, more detailed studies of  $J/\psi$  production in nucleus–nucleus UPCs at the LHC would be extremely useful to put stronger constraints on the nuclear gluon shadowing and gluon distributions in nuclei at small  $x$ .

## 5. Acknowledgements

We would like to thank L. Frankfurt and H. Honkanen for useful discussions and H. Honkanen for providing the EPS09 predictions used in the middle panel of Fig. 3. This work was supported in part by US DOE Contract Number DE-FG02-93ER40771.

## References

- [1] A. Baltz *et al.*, Phys. Rept. 458 (2008) 1-171 [arXiv:0706.3356 [nucl-ex]].
- [2] S. Afanasiev *et al.* [ PHENIX Collaboration ], Phys. Lett. B679 (2009) 321-329.
- [3] E. Abbas *et al.* [ALICE Collaboration], arXiv:1305.1467 [nucl-ex].
- [4] B. Abelev *et al.* [ALICE Collaboration], Phys. Lett. B718 (2013) 1273-1283 [arXiv:1209.3715 [nucl-ex]].
- [5] V. Rebyakova, M. Strikman and M. Zhalov, Phys. Lett. B710 (2012) 647-653 [arXiv:1109.0737 [hep-ph]].
- [6] A. Adeluyi and C. A. Bertulani, Phys. Rev. C85 (2012) 044904 [arXiv:1201.0146 [nucl-th]].
- [7] R. Spital and D. R. Yennie, Phys. Rev. D9 (1974) 138-155.
- [8] A. Aktas *et al.* [H1 Collaboration], Eur. Phys. J. C46 (2006) 585-603 [hep-ex/0510016];  
S. Chekanov *et al.* [ZEUS Collaboration], Eur. Phys. J. C24 (2002) 345-360 [hep-ex/0201043];  
J. J. Aubert *et al.* [EMC Collaboration], Phys. Lett. B89 (1980) 267;  
M. Binkley *et al.*, Phys. Rev. Lett. 48 (1982) 73;  
U. Camerini *et al.*, Phys. Rev. Lett. 35 (1975) 483.
- [9] J. L. Friar and J. W. Negele, Nucl. Phys. A212 (1973) 93-137.  
G. D. Alkhazov, S. L. Belostotsky and A. A. Vorobev, Phys. Rept. 42 (1978) 89-144.
- [10] J. Beringer *et al.* (Particle Data Group), Phys. Rev. D86 (2012) 010001.

- [11] M. Vidovic *et al.*, Phys. Rev. C47 (1993) 2308-2319.
- [12] T. Aaltonen *et al.* [CDF Collaboration], Phys. Rev. Lett. 102 (2009) 242001 [arXiv:0902.1271 [hep-ex]].
- [13] R. Aaij *et al.* [ LHCb Collaboration], arXiv:1301.7084 [hep-ex].
- [14] M. Strikman, M. Tverskoy and M. Zhalov, Phys. Lett. B626 (2005) 72-79 [hep-ph/0505023].
- [15] S. Klein, J. Nystrand, Phys. Rev. C60 (1999) 014903;  
<http://sourceforge.net/projects/upcstarlight>
- [16] H. De Vries, C. W. De Jager, C. De Vries, Atom. Data Nucl. Data Tabl. 36 (1987) 495.
- [17] T. H. Bauer, R. D. Spital, D. R. Yennie and F. M. Pipkin, Rev. Mod. Phys. 50 (1978) 261 [Erratum-ibid. 51 (1979) 407].
- [18] K. J. Golec-Biernat and M. Wusthoff, Phys. Rev. D59 (1998) 014017.
- [19] M. G. Ryskin, Z. Phys. C57 (1993) 89-92.
- [20] S. J. Brodsky, L. Frankfurt, J. F. Gunion, A. H. Mueller and M. Strikman, Phys. Rev. D50 (1994) 3134-3144.
- [21] M. G. Ryskin, R. G. Roberts, A. D. Martin and E. M. Levin, Z. Phys. C76 (1997) 231-239 [hep-ph/9511228].
- [22] P. Hoodbhoy, Phys. Rev. D56 (1997) 388-393 [hep-ph/9611207].
- [23] L. Frankfurt, W. Koepf and M. Strikman, Phys. Rev. D57 (1998) 512-526 [hep-ph/9702216].
- [24] S. -y. Li and X. -N. Wang, Phys. Lett. B527 (2002) 85-91.
- [25] W. -T. Deng, X. -N. Wang and R. Xu, Phys. Lett. B701 (2011) 133-136.
- [26] M. Hirai, S. Kumano and T. -H. Nagai, Phys. Rev. C76 (2007) 065207 [arXiv:0709.3038 [hep-ph]].
- [27] D. de Florian and R. Sassot, Phys. Rev. D69 (2004) 074028.
- [28] K. J. Eskola, H. Paukkunen and C. A. Salgado, JHEP 0904 (2009) 065 [arXiv:0902.4154 [hep-ph]].
- [29] I. Arsene *et al.* [BRAHMS Collaboration], Phys. Rev. Lett. 94 (2005) 032301 [nucl-ex/0401025].
- [30] S. S. Adler *et al.* [PHENIX Collaboration], Phys. Rev. Lett. 98 (2007) 172302 [nucl-ex/0610036].

- [31] L. Frankfurt, V. Guzey and M. Strikman, Phys. Rept. 512 (2012) 255-393 [arXiv:1106.2091 [hep-ph]].
- [32] V. N. Gribov, Sov. Phys. JETP 29 (1969) 483-487 [Zh. Eksp. Teor. Fiz. 56 (1969) 892-901].
- [33] A. Aktas *et. al.* [H1 Collaboration], Eur. Phys. J. C48 (2006) 715-748 and 749-766.
- [34] A. D. Martin, C. Nockles, M. G. Ryskin and T. Teubner, Phys. Lett. B662 (2008) 252-258.
- [35] A. D. Martin, W. J. Stirling, R. S. Thorne and G. Watt, Eur. Phys. J. C63 (2009) 189-285 [arXiv:0901.0002 [hep-ph]].

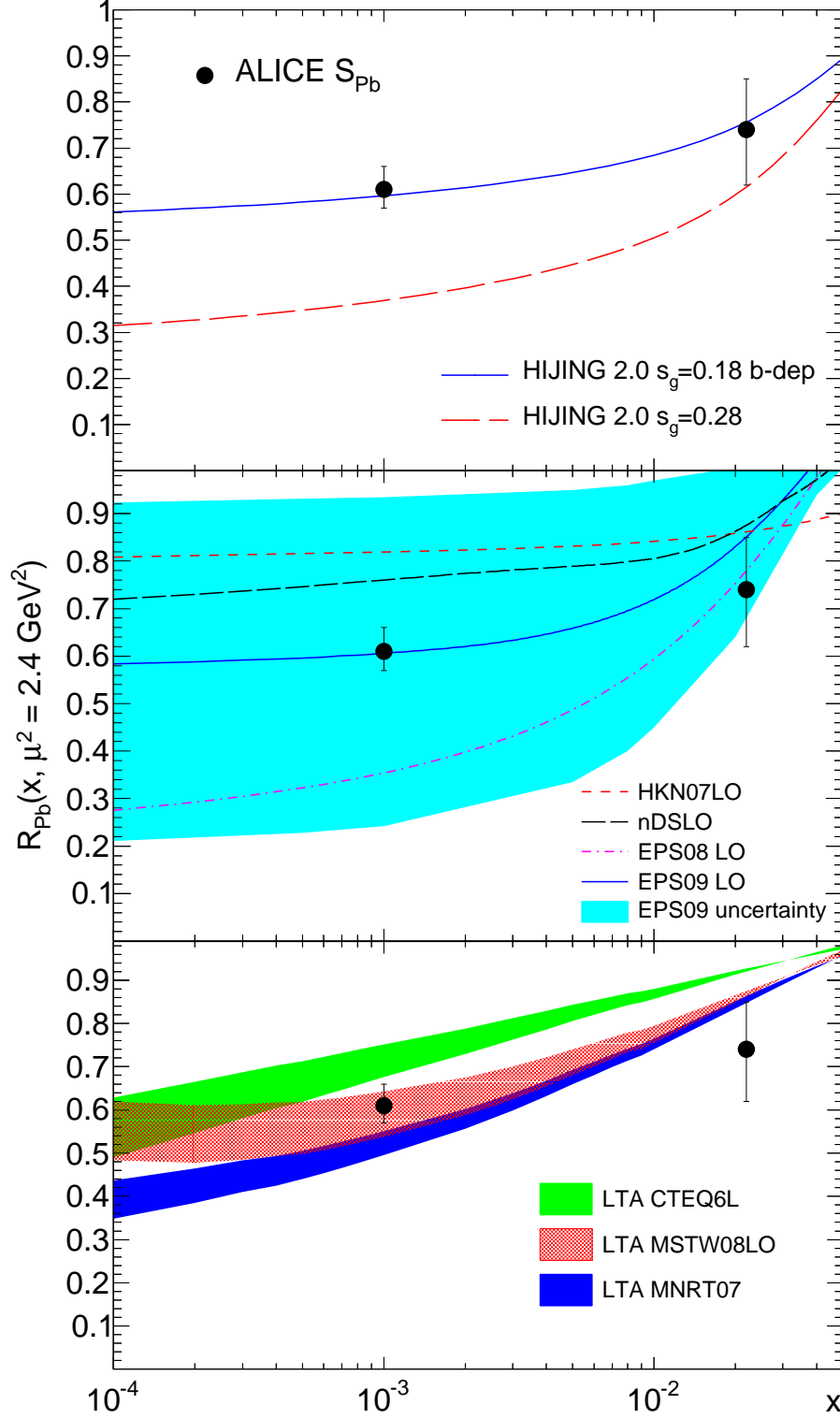


Figure 3: Comparison of the ALICE suppression factors with predictions of the nuclear gluon shadowing in HIJING 2.0 (top), global QCD fits (middle), and in the leading twist approximation (bottom).